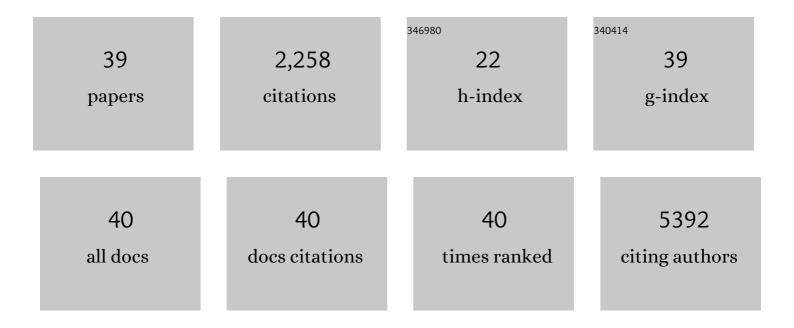
Yuanxi Wang

List of Publications by Year in descending order

Source: https://exaly.com/author-pdf/2710343/publications.pdf Version: 2024-02-01



YHANYI WANG

#	Article	IF	CITATIONS
1	Momentum-Space Spin Antivortex and Spin Transport in Monolayer Pb. Physical Review Letters, 2022, 128, 166601.	2.9	6
2	Photoluminescence Induced by Substitutional Nitrogen in Single-Layer Tungsten Disulfide. ACS Nano, 2022, 16, 7428-7437.	7.3	7
3	SnP ₂ S ₆ : A Promising Infrared Nonlinear Optical Crystal with Strong Nonresonant Second Harmonic Generation and Phase-Matchability. ACS Photonics, 2022, 9, 1724-1732.	3.2	11
4	Enhanced Emission from Defect Levels in Multilayer MoS ₂ . Advanced Optical Materials, 2022, 10, .	3.6	9
5	Illuminating Invisible Grain Boundaries in Coalesced Single-Orientation WS ₂ Monolayer Films. Nano Letters, 2021, 21, 6487-6495.	4.5	26
6	A ReaxFF Force Field for 2D-WS ₂ and Its Interaction with Sapphire. Journal of Physical Chemistry C, 2021, 125, 17950-17961.	1.5	10
7	Theoretical modeling of edge-controlled growth kinetics and structural engineering of 2D-MoSe2. Materials Science and Engineering B: Solid-State Materials for Advanced Technology, 2021, 271, 115263.	1.7	11
8	Nonlinear Dark-Field Imaging of One-Dimensional Defects in Monolayer Dichalcogenides. Nano Letters, 2020, 20, 284-291.	4.5	34
9	Unexpected Near-Infrared to Visible Nonlinear Optical Properties from 2-D Polar Metals. Nano Letters, 2020, 20, 8312-8318.	4.5	22
10	Monolayer Vanadiumâ€Doped Tungsten Disulfide: A Roomâ€Temperature Dilute Magnetic Semiconductor. Advanced Science, 2020, 7, 2001174.	5.6	104
11	Tuning Transport and Chemical Sensitivity via Niobium Doping of Synthetic MoS ₂ . Advanced Materials Interfaces, 2020, 7, 2000856.	1.9	19
12	Modeling for Structural Engineering and Synthesis of Two-Dimensional WSe ₂ Using a Newly Developed ReaxFF Reactive Force Field. Journal of Physical Chemistry C, 2020, 124, 28285-28297.	1.5	20
13	Tuning transport across MoS2/graphene interfaces via as-grown lateral heterostructures. Npj 2D Materials and Applications, 2020, 4, .	3.9	12
14	Multiscale computational understanding and growth of 2D materials: a review. Npj Computational Materials, 2020, 6, .	3.5	89
15	Atomically thin half-van der Waals metals enabled by confinement heteroepitaxy. Nature Materials, 2020, 19, 637-643.	13.3	114
16	Interface-mediated noble metal deposition on transition metal dichalcogenide nanostructures. Nature Chemistry, 2020, 12, 284-293.	6.6	73
17	Geometry and chiral symmetry breaking of ripple junctions in 2D materials. Journal of the Mechanics and Physics of Solids, 2019, 131, 337-343.	2.3	6
18	Dynamics of cleaning, passivating and doping monolayer MoS ₂ by controlled laser irradiation. 2D Materials, 2019, 6, 045031.	2.0	40

#	Article	IF	CITATIONS
19	Multi-scale modeling of gas-phase reactions in metal-organic chemical vapor deposition growth of WSe2. Journal of Crystal Growth, 2019, 527, 125247.	0.7	59
20	Full orientation control of epitaxial <mml:math xmlns:mml="http://www.w3.org/1998/Math/MathML"><mml:msub><mml:mi>MoS</mml:mi><mml:mn>2on hBN assisted by substrate defects. Physical Review B, 2019, 99, .</mml:mn></mml:msub></mml:math 	:m n.x <td>nl:ເສາຮູub></td>	nl :ເສ າຮູub>
21	Defect-Controlled Nucleation and Orientation of WSe ₂ on hBN: A Route to Single-Crystal Epitaxial Monolayers. ACS Nano, 2019, 13, 3341-3352.	7.3	107
22	Probing the origin of lateral heterogeneities in synthetic monolayer molybdenum disulfide. 2D Materials, 2019, 6, 025008.	2.0	6
23	Controllable Edge Exposure of MoS ₂ for Efficient Hydrogen Evolution with High Current Density. ACS Applied Energy Materials, 2018, 1, 1268-1275.	2.5	44
24	Strong exciton regulation of Raman scattering in monolayer <mml:math xmlns:mml="http://www.w3.org/1998/Math/MathML"><mml:msub><mml:mi>MoS</mml:mi><mml:mn>2Physical Review B, 2018, 98, .</mml:mn></mml:msub></mml:math 	:m a.x <td>nl:msub></td>	nl:msub>
25	Research Update: Recent progress on 2D materials beyond graphene: From ripples, defects, intercalation, and valley dynamics to straintronics and power dissipation. APL Materials, 2018, 6, .	2.2	30
26	ReaxFF Reactive Force-Field Study of Molybdenum Disulfide (MoS ₂). Journal of Physical Chemistry Letters, 2017, 8, 631-640.	2.1	126
27	Intervalley scattering by acoustic phonons in two-dimensional MoS2 revealed by double-resonance Raman spectroscopy. Nature Communications, 2017, 8, 14670.	5.8	196
28	Optical identification of sulfur vacancies: Bound excitons at the edges of monolayer tungsten disulfide. Science Advances, 2017, 3, e1602813.	4.7	213
29	Defect Coupling and Sub-Angstrom Structural Distortions in W _{1–<i>x</i>} Mo _{<i>x</i>} S ₂ Monolayers. Nano Letters, 2017, 17, 2802-2808.	4.5	42
30	NanoVelcro: Theory of Guided Folding in Atomically Thin Sheets with Regions of Complementary Doping. Nano Letters, 2017, 17, 6708-6714.	4.5	8
31	Intricate Resonant Raman Response in Anisotropic ReS ₂ . Nano Letters, 2017, 17, 5897-5907.	4.5	66
32	Theory of Finite-Length Grain Boundaries of Controlled Misfit Angle in Two-Dimensional Materials. Nano Letters, 2017, 17, 5297-5303.	4.5	20
33	Observation of a Quasi-ordered Structure in Monolayer W x Mo (1-x) S 2 Alloys. Microscopy and Microanalysis, 2016, 22, 1548-1549.	0.2	1
34	Lowâ€Temperature Solution Synthesis of Few‣ayer 1T ′â€MoTe ₂ Nanostructures Exhibiti Lattice Compression. Angewandte Chemie - International Edition, 2016, 55, 2830-2834.	^{ng} 7.2	84
35	Spontaneous Formation of Atomically Thin Stripes in Transition Metal Dichalcogenide Monolayers. Nano Letters, 2016, 16, 6982-6987.	4.5	48
36	Lowâ€Temperature Solution Synthesis of Few‣ayer 1T ′â€MoTe 2 Nanostructures Exhibiting Lattice Compression. Angewandte Chemie, 2016, 128, 2880-2884.	1.6	22

#	Article	IF	CITATIONS
37	Non-oxidative intercalation and exfoliation of graphite by BrÃ,nsted acids. Nature Chemistry, 2014, 6, 957-963.	6.6	175
38	Extraordinary Second Harmonic Generation in Tungsten Disulfide Monolayers. Scientific Reports, 2014, 4, 5530.	1.6	262
39	Reversible Intercalation of Hexagonal Boron Nitride with BrÃ,nsted Acids. Journal of the American Chemical Society, 2013, 135, 8372-8381.	6.6	88